

On the elemental effect of AlCoCrCuFeNi high-entropy alloy system

Chung-Chin Tung ^a, Jien-Wei Yeh ^{a,*}, Tao-tsung Shun ^b, Swe-Kai Chen ^c,
Yuan-Sheng Huang ^{a,d}, Hung-Cheng Chen ^e

^a Department of Materials Science and Engineering, National Tsing Hua University, Hsinchu 300, Taiwan

^b Department of Materials Science and Engineering, Feng-Chia University, Taichung 40724, Taiwan

^c Materials Science Center, National Tsing Hua University, Hsinchu 300, Taiwan

^d Department of Mechanical and electronic engineering, Shaoguan University, Shaoguan City, Guangdong 512005, China

^e Materials Research Laboratories, Industrial Technology Research Institute, Chutung 310, Taiwan

Received 15 October 2005; accepted 29 March 2006

Available online 27 April 2006

Abstract

The AlCoCrCuFeNi high-entropy alloy system was synthesized using a well-developed arc melting and casting method. Their elemental effect on microstructures and hardness was investigated with X-ray diffraction, scanning electron microscopy and Vickers hardness testing. The alloys exhibit quite simple FCC and BCC solid solution phases. Co, Cu and Ni elements enhance the formation of the FCC phase while Al and Cr enhance that of the BCC phase in the alloy system. BCC phases form a spinodal structure during cooling. Copper tends to segregate at the interdendrite region and forms a Cu-rich FCC phase. Low copper content renders the interdendrite as a thin film and the as-cast structure like recrystallized grain structure. The formation of BCC phases significantly increases the hardness level of the alloy system. The strengthening mechanism is discussed.

© 2006 Elsevier B.V. All rights reserved.

Keywords: High-entropy alloy; Elemental effect; Microstructure; Hardness

1. Introduction

High-entropy alloys were developed in recent years by Yeh et al. [1,2]. They define these alloys to have at least five principal elements with the concentration of each principal element being between 35 and 5 at.%. There are a huge number of alloys belonging to this alloy regime. Solid solutions with multi-principal elements have been generally found to be more stable than intermetallic compounds at elevated temperatures due to their large entropies of mixing. Moreover, nano-precipitation is easy to obtain even in the as-cast state because of the sluggish diffusion of atoms in a matrix with multi-principal elements [3–7]. Similar findings of simple solid solution phases in the as-cast alloys based on FeCrMnNiCo

with further addition of other elements were also reported by Cantor et al. [8]. The promising properties of high-entropy alloys offer the potential to be used in many applications, such as tools, molds, dies, mechanical parts and furnace parts, which require high strength, thermal stability, and wear and oxidation resistance, with application temperatures up to 800 °C. In addition, coating technology will further expand the application of such alloys to functional films, such as hard-facing of golf heads and rollers, diffusion barriers, and soft magnetic films [2–11].

Among the alloys investigated, $\text{Al}_x\text{CoCrCuFeNi}$ ($x=0$ to 3 in molar ratio) is an interesting system which has a wide range of microstructure and properties as aluminum content is varied [7,12]. For a further understanding of this alloy system and to facilitate the alloy design, each element is varied with two levels, that is, 0.5 and 1.0 in molar ratio in this study so that their microstructure and hardness could be compared to see the effect of different elements. In addition, some general trends of high-entropy alloys are summarized.

* Corresponding author.

E-mail address: jwyeh@mx.nthu.edu.tw (J.-W. Yeh).

2. Experimental details

The AlCoCrCuFeNi high-entropy alloy system was prepared by arc melting and casting method. The method followed the same procedure as described in Ref. [4]. The alloy specimens were polished and etched with aqua regia for observation under an optical microscope and a scanning electron microscope (SEM, JEOL JSM-5410). The chemical compositions of different phases were analyzed by SEM energy dispersive spectrometry (EDS). An X-ray diffractometer (XRD, Rigaku ME510-FM2, Tokyo, Japan) was used for the identification of a crystalline structure with the 2θ scan ranging from 20° to 100° at a speed of $1^\circ/\text{min}$. The typical radiation condition was 30 kV and 20 mA with a copper target. Hardness measurements were conducted using a Vickers hardness tester (Matsuzawa Seiki MV-1) under a load of 49 N and at a loading speed of $70 \mu\text{m}/\text{s}$ for 20 s .

3. Results and discussion

3.1. X-ray diffraction analysis

The X-ray diffraction patterns of the AlCoCrCuFeNi alloy system with each element varied at 0.5 and 1.0 in molar ratio are shown in Fig. 1. The crystal structure of as-cast equimolar AlCoCrCuFeNi alloy is identified to be of simple solid-solution structures based on FCC and BCC structures. By a reduction of aluminum content, $\text{Al}_{0.5}\text{CoCrCuFeNi}$ alloy is of the FCC structure. By a reduction of copper content $\text{AlCoCrCu}_{0.5}\text{FeNi}$ is of the BCC structure. Except for these two cases, other four alloys of different element reductions are all composed of FCC and BCC phases. Comparing the relative X-ray intensity of the strongest peaks of FCC and BCC phases with that of the base alloy AlCoCrCuFeNi, it can be seen that Co, Cu and Ni enhance the FCC phase formation while Al and Cr favor the BCC phase formation. This leads to the fact that Co, Cu and Ni are FCC formers while Al and Cr are BCC formers, as found in steels. It is also seen that ordering occurs in BCC phases of AlCoCrCuFeNi, $\text{AlCo}_{0.5}\text{CrCuFeNi}$, $\text{AlCoCr}_{0.5}\text{CuFeNi}$, $\text{AlCoCrCu}_{0.5}\text{FeNi}$, $\text{AlCoCrCuFe}_{0.5}\text{Ni}$, and $\text{AlCoCrCuFeNi}_{0.5}$ as an ordered peak appears at around 31° in their XRD patterns. This relates with the spinodal

Table 1
Microstructure, lattice constants and hardness

Alloys	Microstructure	FCC lattice constant (\AA)	BCC lattice constant (\AA)	Hardness (HV)
AlCoCrCuFeNi	FCC+BCC	3.60	2.87	420
$\text{Al}_{0.5}\text{CoCrCuFeNi}$	FCC	3.59	—	208
$\text{AlCo}_{0.5}\text{CrCuFeNi}$	FCC+BCC	3.62	2.87	473
$\text{AlCoCr}_{0.5}\text{CuFeNi}$	FCC+BCC	3.61	2.87	367
$\text{AlCoCrCu}_{0.5}\text{FeNi}$	BCC	—	2.87	458
$\text{AlCoCrCuFe}_{0.5}\text{Ni}$	FCC+BCC	3.61	2.87	418
$\text{AlCoCrCuFeNi}_{0.5}$	FCC+BCC	3.63	2.87	423

decomposition of the BCC phase which forms at high temperatures and decomposes into disordered BCC (A2) and ordered BCC (B2) phases [7]. Since Al is the strongest BCC former and enhances the ordering of BCC phase, all alloys except $\text{Al}_{0.5}\text{CoCrCuFeNi}$ have the ordered BCC phase.

The lattice constants of the phases in all the alloys are summarized in Table 1. It can be seen that the lattice constant of the FCC phase decreases as the content of Al decreases from 1.0 to 0.5, whereas it increases as the content of each of Co, Cr, Fe and Ni decreases from 1.0 to 0.5. On the other hand, the lattice constant of the BCC phase remains the same to the second decimal position as the content of each of Co, Cr, Cu, Fe and Ni decreases from 1.0 to 0.5. This is reasonable since the lattice constant is relevant to the atomic size of all constituent atoms in the unit cell. Since the size of Al, 1.46 \AA (Table 2), is the biggest of six elements, it leads to the fact that the lattice constant of the FCC phase decreases as the aluminum content decreases and increases as the content of other five elements increases. Moreover, since the size of Ni is the smallest, 1.245 \AA (Table 2), the lattice constant of the FCC phase is the largest as the content of Ni decreases from 1.0 to 0.5. As for the lattice constant of the BCC phase, since the BCC phase already includes a large part of the strongest BCC former, Al, and significantly expands its unit cell, the influence of other smaller elements on the lattice constant becomes very small.

3.2. Hardness

The hardness values of the alloys are shown in Table 1. $\text{Al}_{0.5}\text{CoCrCuFeNi}$ has a hardness of 208 HV which is significantly smaller than that of other alloys. Since $\text{Al}_{0.5}\text{CoCrCuFeNi}$ is composed of the FCC phase whereas other alloys contain more BCC phase, e.g. $\text{AlCoCrCu}_{0.5}\text{FeNi}$ is almost composed of the BCC phase, it indicates that the BCC phase is much stronger than the FCC phase. A similar phenomenon was also reported in the study on $\text{Al}_x\text{CoCrCuFeNi}$ ($x=0$ to 3 in molar ratio) [12]. The reason for the better strength of the BCC phase as compared to the FCC phase can be explained with the basic structure factor and solution hardening mechanism. For the basic structure factor, a slip along the closest packing planes $\{110\}$ in the BCC structure is more difficult than those along $\{111\}$ in the FCC structure since $\{110\}$ planes are less dense and more irregular and thus possess a smaller interplanar spacing and higher lattice friction for dislocation motion than $\{111\}$.

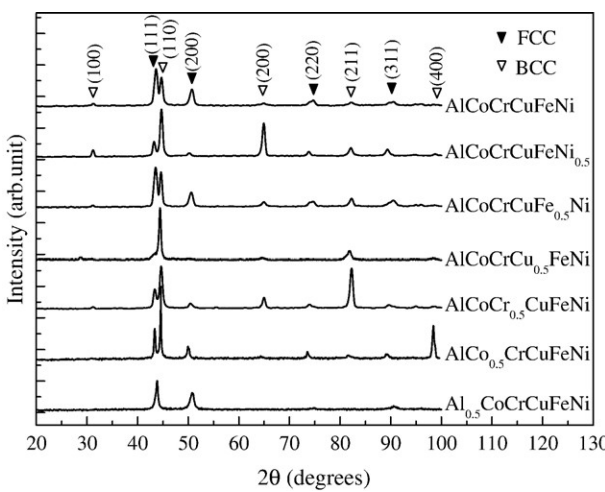


Fig. 1. XRD patterns of the experimental alloys in the as-cast condition.

Table 2
Atomic size of the experimental elements

Element	Al	Cu	Ni	Co	Fe	Cr
Atomic size (\AA)	1.43	1.28	1.245	1.25	1.24	1.25

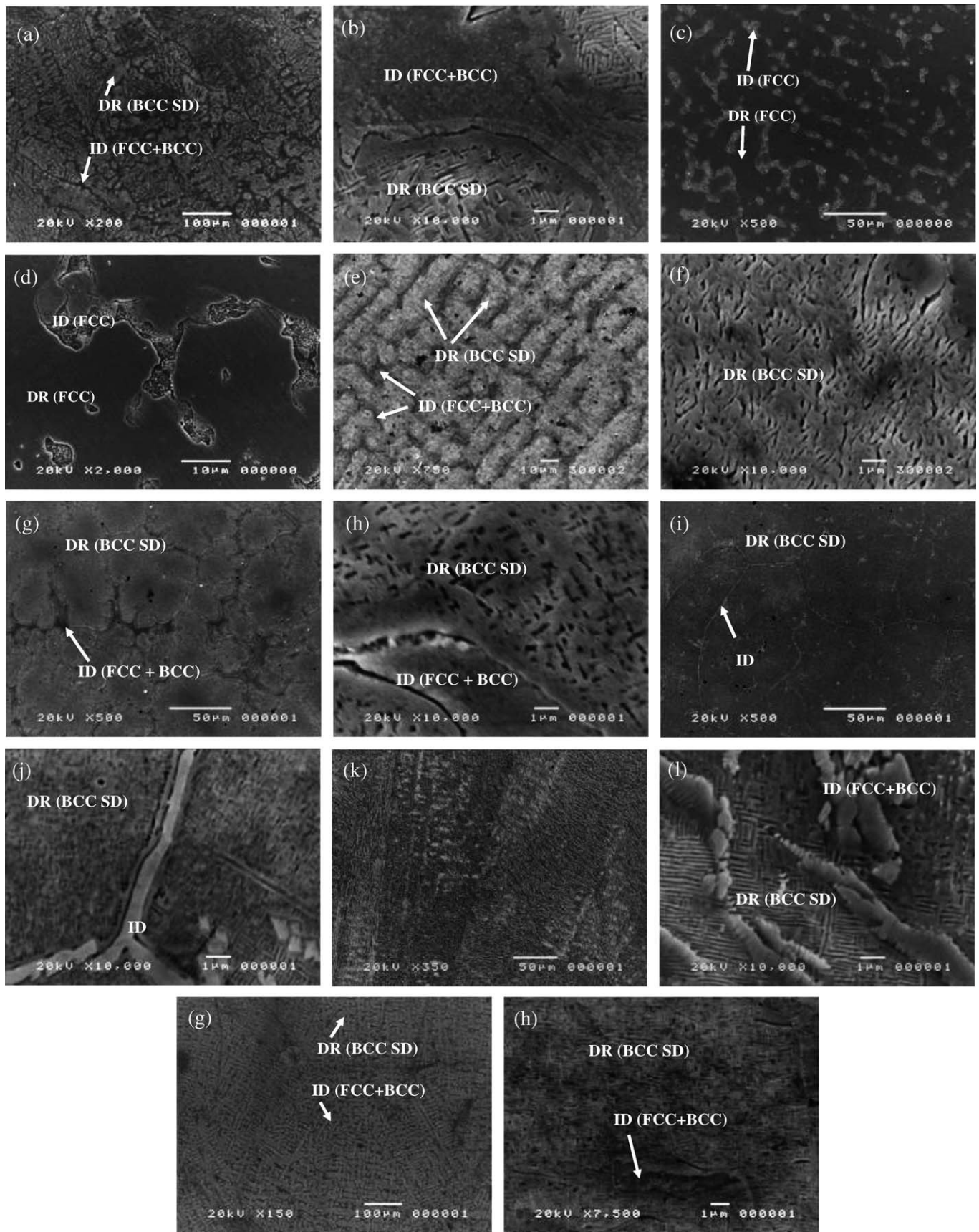


Fig. 2. SEM microstructures of (a) and (b) AlCoCrCuFeNi, (c) and (d) Al_{0.5}CoCrCuFeNi, (e) and (f) AlCo_{0.5}CrCuFeNi, (g) and (h) AlCoCr_{0.5}CuFeNi, (i) and (j) AlCoCrCu_{0.5}FeNi, (k) and (l) AlCoCrCuFe_{0.5}Ni, and (m) and (n) AlCoCrCuFeNi_{0.5} (DR: dendrite, ID: interdendrite, SD: spinodal decomposition).

Table 3
Chemical composition of dendrite and interdendrite in atomic percentage

Alloy		Al	Co	Cr	Cu	Fe	Ni
AlCoCrCuFeNi	Nominal	16.6	16.6	16.6	16.6	16.6	16.6
	Dendrite	15	20	25	7	21	12
	Interdendrite	14	9	7	50	8	12
Al _{0.5} CoCrCuFeNi	Nominal	9.0	18.1	18.1	18.1	18.1	18.1
	Dendrite	7	22	19	10	24	18
	Interdendrite	13	14	11	28	14	19
AlCo _{0.5} CrCuFeNi	Nominal	18.1	9.0	18.1	18.1	18.1	18.1
	Dendrite	20	10	23	12	17	18
	Interdendrite	11	5	6	48	14	16
AlCoCr _{0.5} CuFeNi	Nominal	18.1	18.1	9.0	18.1	18.1	18.1
	Dendrite	26	17	9	12	17	19
	Interdendrite	21	11	6	35	11	16
AlCoCrCu _{0.5} FeNi	Nominal	18.1	18.1	18.1	9.0	18.1	18.1
	Dendrite	17	18	19	8	18	20
AlCoCrCuFe _{0.5} Ni	Nominal	18.1	18.1	18.1	18.1	9.0	18.1
	Dendrite	24	16	16	14	9	21
	Interdendrite	14	19	15	27	7	18
AlCoCrCuFeNi _{0.5}	Nominal	18.1	18.1	18.1	18.1	18.1	9.0
	Dendrite	20	20	21	8	21	10
	Interdendrite	16	16	17	30	13	8

planes in the atomic scale [12–15]. For hardening the solution, the incorporation of the strongest binding element Al and highest melting point element Cr into the BCC lattice increases the Young's modulus and slip resistance. The atomic size difference is also a factor and reflected by the largest atom Al since more Al would increase the lattice distortion and resist the slip [14–16]. The solute-strengthening effect of Cr might also be reflected in the hardness comparison between AlCoCr_{0.5}CuFeNi and AlCoCrCuFeNi. Although the former has a relatively higher amount of BCC phase than the latter as seen in their XRD patterns, its hardness is still smaller than that of the latter. This is because less Cr in BCC phase would cause a lower Young's modulus.

3.3. SEM analyses

Fig. 2 shows the as-cast SEM microstructures of the AlCoCrCuFeNi alloy system. Typical cast dendrite and interdendrite structures (defined as DR and ID in the figures, respectively) are observed in these alloys. However, the morphology of dendrite and interdendrite is diverse in this alloy system indicating a difference in composition could have a large effect on the growth behavior of dendrites. Table 3 shows the chemical composition of dendrite and interdendrite analyzed by EDS. Copper segregation to interdendrite is typically seen in this alloy system. This can be explained with the bonding energy between copper and each of cobalt, chromium, iron and nickel is 6, 12, 13 and 4 kJ/mol [17], it leads to the fact that copper dislikes living in dendrite with more cobalt, chromium, iron, and nickel concentration. Combined with the XRD analysis, both the dendrite and interdendrite of Al_{0.5}CoCrCuFeNi (Fig. 2c and d) are of one simple FCC phase, respectively. The dendrites of AlCoCrCuFeNi (Fig. 2a and b), AlCo_{0.5}CrCuFeNi (Fig. 2e and f), AlCoCr_{0.5}CuFeNi (Fig. 2g and h), AlCoCrCu_{0.5}FeNi (Fig. 2i and j), AlCoCrCuFe_{0.5}Ni (Fig. 2k and l), and AlCoCrCuFeNi_{0.5} (Fig. 2m and n) are of BCC phase which further decompose into spinodal modulated structures while the interdendrites are composed of FCC and/or BCC phases, respectively. It is noted that the dendrite of AlCoCrCu_{0.5}FeNi (Fig. 2i and j) appears as a grain structure and its interdendrite is a thin film

along grain boundaries. The formation of this boundary film is reasonable since the Cu content is reduced by a half and thus the Cu-rich phase decreases in amount drastically. Their grains are of the BCC phase as revealed by the XRD analysis. Such as-cast grain structure is similar to that of pure metal which implies that the composition of AlCoCrCu_{0.5}FeNi has a very narrow solidification freeze range. This is quite unique for an alloy composition that contains a large number of principal elements.

4. Conclusions

The AlCoCrCuFeNi alloy system with each element varied at 0.5 and 1.0 in molar ratio exhibits simple FCC and BCC solid solution phases. Co, Cu, and Ni elements enhance FCC phase formation while Al and Cr enhance BCC phase formation in the alloy system. Their phase tendency is similar to that found in steel. BCC phases of the alloy system tend to form a spinodal structure during cooling. Copper tends to segregate at the interdendrite region. Low copper content reduces the volume fraction of the interdendrite and allows the as-cast structure to appear like a recrystallized grain structure. The formations of the BCC phase result in a significant increase of hardness. The strengthening is explained based on the basic structure factor and solution hardening mechanism.

Acknowledgments

The authors gratefully acknowledge the financial support for this research by the National Science Council of Taiwan under grant no. NSC-91-2120-E-007-007 and the Ministry of Economic Affairs of Taiwan under grant no. 92-CE-17-A-08-S1-0003.

References

- [1] S. Ranganathan, Current Sci. 85 (2003) 1404–1406.
- [2] J.W. Yeh, S.K. Chen, S.J. Lin, J.Y. Gan, T.S. Chin, T.T. Shun, C.H. Tsau, S.Y. Chang, Adv. Eng. Mater. 6 (2004) 299–303.
- [3] R.A. Swalin, Thermodynamics of Solids, in: E. Burke, B. Chalmers, J.A. Krumhansl (Eds.), ed. 2, John Wiley and Sons, New York, NY, 1991, pp. 21–87.
- [4] P.K. Huang, J.W. Yeh, T.T. Shun, S.K. Chen, Adv. Eng. Mater 6 (2004) 74–78.
- [5] C.Y. Hsu, J.W. Yeh, S.K. Chen, T.T. Shun, Metall. Mater. Trans., A, Phys. Metall. Mater. Sci. 35A (2004) 1465–1469.
- [6] J.W. Yeh, S.K. Chen, J.Y. Gan, S.J. Lin, T.S. Chin, T.T. Shun, C.H. Tsau, S.Y. Chang, Metall. Mater. Trans., A, Phys. Metall. Mater. Sci. 35A (2004) 2533–2536.
- [7] C.J. Tong, S.K. Chen, J.W. Yeh, T.T. Shun, C.H. Tsau, S.J. Lin, S.Y. Chang, Metall. Mater. Trans., A, Phys. Metall. Mater. Sci. 36A (2005) 881–893.
- [8] B. Cantor, I.T.H. Chang, P. Knight, A.J.B. Vincent, Metall. Mater. Trans., A, Phys. Metall. Mater. Sci. 375–377 (2004) 213–218.
- [9] T.K. Chen, T.T. Shun, J.W. Yeh, M.S. Wong, Surf. Coat. Technol. 188–189 (2004) 193–200.
- [10] Y. Chen, T. Duval, U.D. Hung, J.W. Yeh, H.C. Shih, Corros. Sci. 47 (2005) 2257–2279.
- [11] Y.Y. Chen, U.D. Hung, H.C. Shih, J.W. Yeh, T. Duval, Corros. Sci. 47 (2005) 2679–2699.
- [12] C.J. Tong, M.R. Chen, S.K. Chen, J.W. Yeh, T.T. Shun, S.J. Lin, S.Y. Chang, Metall. Mater. Trans., A, Phys. Metall. Mater. Sci. 36A (2005) 1263–1271.

- [13] R.E. Reed-Hill, R. Abbaschian, Physical Metallurgy Principles, Third edition, PWS-KENT Publishing Company, Boston, 1994, pp. 140–146.
- [14] T. Courtney, Mechanical Behavior of Materials, McGraw-Hill, New York, 1990, pp. 173–184.
- [15] G.E. Dieter, Mechanical Metallurgy, SI Metric Editions, McGraw-Hill Book Company, New York, 1988, pp. 117–121.
- [16] G.E. Dieter, Mechanical Metallurgy, SI Metric Editions, McGraw-Hill Book Company, New York, 1988, pp. 208–212.
- [17] F.R. de Boer, R. Boom, W.C.M. Mattens, A.R. Miedema, A.K. Nissen, Cohesion in Metals, Elsevier Science Publishing Company, 1989.